Nonreciprocal phonon blockade based on a spinning optomechanical system

Xiao Feng(冯潇)[1,2], Jin-Xiao Cai(蔡金枭)[1], Ming-Hao Cai(蔡明皓)[1,3], Jing-Jing Zhang(张京京)[1], Jia-Neng Li(李嘉能)[1], Yu-Ming Huang(黄聿铭)[1], and Shan-Shan Chen(陈珊珊)[1,†]

[1] *School of Electronic Science and Engineering, Chongqing University of Posts and Telecommunications, Chongqing* 400065, *China*
[2] *Chongqing Key Laboratory of Optoelectronic Information Sensing and Transmission Technology, Chongqing University of Posts and Telecommunications, Chongqing* 400065, *China*
[3] *School of Intelligent Manufacturing, Sichuan University of Arts and Science, Dazhou* 635000, *China*

(Received 17 November 2025; revised manuscript received 20 January 2026; accepted manuscript online 6 February 2026)

Phonon blockade (PB) has attracted extensive attention due to its potential application in the development of phonon-based quantum information processing, single-phonon sources, and other single-phonon quantum devices. In this paper, we investigate the generation of nonreciprocal PB in a spinning optomechanical system that consists of a single mechanical oscillator and two rotating optical resonators. The nonreciprocal behavior is induced by the Sagnac effect and the PB originates from the strong anharmonicity of the eigenstates. We find that the frequency detuning region where the nonreciprocal PB occurs can be broadened as the angular velocities of the two optical resonators increase. The nonreciprocal PB can be modulated by the optomechanical coupling strength and the frequency detuning between the mechanical mode and the pump field. We find that the nonreciprocal PB can still exist even when the mechanical thermal phonon numbers are considered. This work provides a new way to manipulate quantum nonreciprocal devices, which are crucial elements in acoustic signal processing and precision measurement.

Keywords: optomechanical system, phonon blockade,nonreciprocity, Sagnac effect

PACS: 42.50.–p, 42.50.Dv , 42.50.Lc

DOI: 10.1088/1674-1056/ae42b5 **CSTR:** 32038.14.CPB.ae42b5

CPB Online In Press

1. Introduction

The mechanical resonator is an important macroscopic object in the field of quantum optics. Its tunable coupling to various physical systems, including the superconducting qubit,[1–3] the nitrogen-vacancy center in diamond,[4] and the optomechanical system,[5–10] is of great interest. Quantum effects of mechanical resonators demonstrate significant potential in quantum information processing and ultrasensitive measurements. Phonon blockade (PB), a phenomenon where the second phonon is blockaded when the first one is absorbed, is one of the important quantum effects of the mechanical oscillator. This concept comes from the photon blockade in cavity QED systems,[11] A PB enables the realization of an ideal single-phonon source, which has been observed in a qubit-coupled nanomechanical resonator,[12,13] a two-level defect,[14] and an optomechanical system,[15,16] Optomechanical systems,[17,18] where a mechanical oscillator is coupled to a cavity field via the radiation-pressure force, serve as a powerful tool to control the mechanical freedom and can be regarded as an ideal platform for investigating the PB. To date, the investigation of the PB based on an optomechanical system has made great achievements.[19–23]

Nonreciprocal devices that permit signal transmission in one direction while blocking it in the opposite direction are essential for quantum technologies including noise-resistant quantum processors, sensors, and chiral quantum networks. Nonreciprocal devices have been realized through various effects, for example, the magneto-optical Faraday rotation effect,[24–27] the modulation of the refractive index,[28–30] and the Hall effect.[31] Phononic nonreciprocal devices have emerged as indispensable resources for the construction of phonon-based quantum networks and sensitive measurements. Many different phononic nonreciprocal devices have been implemented in optomechanical systems,[32–38] such as nonreciprocal mechanical squeezing,[32–34] nonreciprocal phonon lasers,[35,36] and nonreciprocal ground-state cooling of phonon modes.[37,38]

However, existing phononic nonreciprocal devices primarily focus on manipulating macroscopic phonon flows — such as transmission direction,[39] amplification (lasing),[35,36] or cooling efficiency,[37,38] — while the nonreciprocal control of intrinsic phonon quantum statistics remains a less explored yet vital frontier for advanced quantum phononics. Achieving directional control over quantum-statistical phenomena like PB would enable novel devices such as chiral single-phonon sources and phonon routers. Compared to mature nonreciprocal photon blockade schemes that often rely on strong magnetic fields or complex optical nonlinearities,[40–42] imple-

†Corresponding author. E-mail: chenss@cqupt.edu.cn

© 2026 Chinese Physical Society and IOP Publishing Ltd. All rights, including for text and data mining, AI training, and similar technologies, are reserved.

menting a compact, tunable, and integrated nonreciprocal PB platform is highly desirable.

A recent scheme using atomic-cavity coupling demonstrated nonreciprocal PB,[22] but its reliance on precise atomic control and cryogenic conditions complicates integration. In contrast, our dual-spinning-cavity scheme eliminates atomic systems entirely, working purely within an optomechanical framework. This simplifies the structure and enhances integrability with photonic platforms. Furthermore, compared to the solid-state color center scheme, where phonon nonlinearity is engineered via spin–phonon coupling combined with microwave control and phononic spin–orbit interaction,[43] our approach represents a fundamentally distinct optomechanical pathway. Our scheme's nonlinearity stems from an all-optically tunable quadratic optomechanical interaction. While the spin-based scheme inherently operates without optical cavity noise, our scheme operates in an all-optical domain, leveraging the tunability of quadratic optomechanical coupling which can be controlled in situ via laser power, offering a direct route to photonic integration without requiring cryogenic atomic or spin systems.

Here we propose how to realize the nonreciprocal PB in a spinning device composed of two spinning optical resonators and a mechanical oscillator. The nonlinear interaction between phonons, which is induced by the optomechanical coupling via the radiation-pressure force and the tunneling coupling between two optical resonators, results in the emergence of the anharmonic energy level of the system, and the PB can be obtained. The rotation-induced Sagnac effect is the origin of the nonreciprocity. We discuss the second-order correlation function of the mechanical mode which is used to characterize the phonon statistical properties and the results show that the frequency detuning range where nonreciprocal PB exists can be broadened greatly, and the PB can be modulated by the driving field of the optical resonator and the tunneling coupling strength. We also investigate the effect of photon states on the nonreciprocal phonon blockade, and it is found that the rotation-induced Sagnac frequency shift leads to the difference of the phonon statistical properties of the mechanical mode in n-photon states. The nonreciprocal PB will not disappear when the mechanical thermal phonon numbers are present.

2. Optomechanical system

As shown in Fig. 1, we consider a spinning optomechanical device,[44] where two spinning whispering-gallery mode (WGM) microresonators both couple to a mechanical oscillator, and there is a tunneling coupling between these two WGM oscillators. When a driving field transports from port 1 to port 2, the optical resonators 1 and 2 support counterclockwise (CCW) and clockwise (CW) WGMs, respectively. Conversely, the CW and CCW WGMs appear in the optical resonators 1 and 2, respectively, for a driving field transporting from port 2 to port 1. Two WGM resonators both spin CCW at the same angular velocities Ω. The optical mode in the WGM resonators experiences a Fizeau shift,[45] due to the Sagnac effect, i.e., $\omega_0 \to \omega_0 + \Delta_{\rm F}$, with

$$\Delta_{\rm F} = \frac{n_1 r \Omega \omega_0}{c}\left(1 - \frac{1}{n_1} - \frac{\lambda}{n_1}\frac{{\rm d}n_1}{{\rm d}\lambda}\right), \tag{1}$$

where $\omega_0 = 2\pi c/\lambda$ is the optical resonance frequency of the WGM resonator without spinning, c (λ) is the speed (wavelength) of light in vacuum, n_1 and r are the refractive index and the radius of the WGM resonators, respectively. The dispersion term ${\rm d}n_1/{\rm d}\lambda$ which characterizes the relativistic origin of the Sagnac effect is relatively small in typical materials ($\sim 1\%$).[45,46] We consider the CCW rotation of two WGM resonators. $\Delta_{\rm F} < 0$ ($\Delta_{\rm F} > 0$) represents the case where the driving field is transmitted from port 1 (2), where the driving light propagates along (against) the spinning direction of the WGM resonators. The resonance frequency of the optical mode is $\omega_0 - |\Delta_{\rm F}|(\omega_0 + |\Delta_{\rm F}|)$ for $\Delta_{\rm F} < 0$ ($\Delta_{\rm F} > 0$).

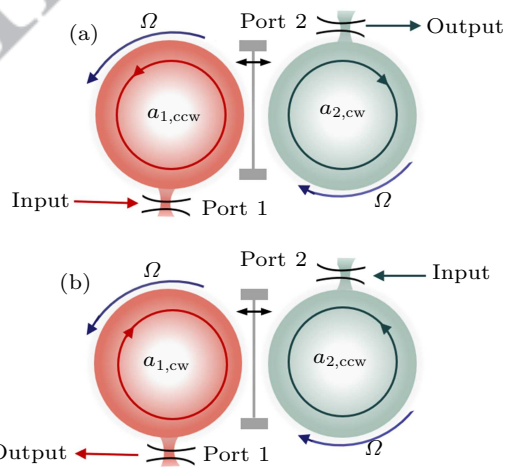


Fig. 1. Schematic of the system where two tunnel-coupled spinning whispering-gallery mode (WGM) microresonators simultaneously couple to a mechanical oscillator. Here the mechanical oscillator is placed between two WGM microresonators.

The Hamiltonian of the system can be given as

$$\begin{aligned} H_0 =\ & (\omega_0 - |\Delta_{\rm F}|)(a^\dagger_{1,\rm ccw}a_{1,\rm ccw} + a^\dagger_{2,\rm cw}a_{2,\rm cw}) \\ & + (\omega_0 + |\Delta_{\rm F}|)(a^\dagger_{1,\rm cw}a_{1,\rm cw} + a^\dagger_{2,\rm ccw}a_{2,\rm ccw}) \\ & + \frac{1}{2}\omega_m(q^2 + p^2) \\ & + \sum_{j=1,2}\sum_{k=\rm cw,ccw}(-1)^j g_0 q a^\dagger_{j,k}a_{j,k} \\ & + J(a_{1,\rm ccw}a^\dagger_{2,\rm cw} + a_{1,\rm cw}a^\dagger_{2,\rm ccw} + {\rm H.c.}), \end{aligned} \tag{2}$$

where $a_{j,k}$ ($j = 1,2$, $k = $ cw, ccw) is the annihilation operator of the optical mode. q and p are the displacement and momentum operators of the mechanical oscillator with frequency ω_m, respectively. g_0 is the single-photon coupling strength between the mechanical mode and any one of the two WGM

CPB Online In-Press

optical modes. J is the tunneling coupling strength between the two WGM optical modes.

The Hamiltonian in Eq. (2) can be diagonalized as

$$\begin{aligned} H_0 &= \omega_{1+}(q)a^{\dagger}_{\mathrm{L},+}a_{\mathrm{L},+} + \omega_{1-}(q)a^{\dagger}_{\mathrm{L},-}a_{\mathrm{L},-} \\ &+ \omega_{2+}(q)a^{\dagger}_{\mathrm{R},+}a_{\mathrm{R},+} + \omega_{2-}(q)a^{\dagger}_{\mathrm{R},-}a_{\mathrm{R},-} \\ &+ \frac{1}{2}\omega_m(q^2+p^2), \end{aligned} \tag{3}$$

where the normal mode basis

$$\begin{aligned} a_{\mathrm{L},\pm} &= \frac{1}{D_{\pm}}[Ja_{1,\mathrm{ccw}} + (g_0 q + \sqrt{J^2+(g_0 q)^2})a_{2,\mathrm{cw}}], \\ a_{\mathrm{R},\pm} &= \frac{1}{D_{\pm}}[Ja_{1,\mathrm{cw}} + (g_0 q + \sqrt{J^2+(g_0 q)^2})a_{2,\mathrm{ccw}}], \end{aligned} \tag{4}$$

with

$$D^2_{\pm} = J^2 + (g_0 q \pm \sqrt{J^2+(g_0 q)^2}), \tag{5}$$

and the eigenfrequencies

$$\omega_{j\pm}(q) = \omega_0 + (-1)^j|\Delta_{\mathrm{F}}| \pm \sqrt{J^2+(g_0 q)^2}. \tag{6}$$

We assume $|J| \gg g_0 q$ and, using the approach in Refs. [47–49], a Taylor expansion of the eigenfrequencies can be used as

$$\omega_{j\pm}(q) \approx \omega_{j\pm} \pm \frac{g_0^2 q^2}{2J}, \tag{7}$$

where we have denoted $\omega_{j\pm} = \omega_0 + (-1)^j|\Delta_{\mathrm{F}}| \pm J$. We define

$$g = g_0^2/(2J), \tag{8}$$

the Hamiltonian in Eq. (3) can be written as

$$\begin{aligned} H_0 &\approx (\omega_{1+} + gq^2)a^{\dagger}_{\mathrm{L},+}a^{\dagger}_{\mathrm{L},+} + (\omega_{2+} + gq^2)a^{\dagger}_{\mathrm{R},+}a^{\dagger}_{\mathrm{R},+} \\ &+ (\omega_{1-} - gq^2)a^{\dagger}_{\mathrm{L},-}a^{\dagger}_{\mathrm{L},-} + (\omega_{2-} - gq^2)a^{\dagger}_{\mathrm{R},-}a^{\dagger}_{\mathrm{R},-} \\ &+ \frac{1}{2}\omega_m(q^2+p^2), \end{aligned} \tag{9}$$

where quasi-static normal optical modes

$$\begin{aligned} a_{\mathrm{L},\pm} &\approx (a_{1,\mathrm{ccw}} \pm a_{2,\mathrm{cw}})/\sqrt{2}, \\ a_{\mathrm{R},\pm} &\approx (a_{1,\mathrm{cw}} \pm a_{2,\mathrm{ccw}})/\sqrt{2}. \end{aligned} \tag{10}$$

At present, numerous schemes[15,21,50,51] have been proposed to show that quadratic optomechanical coupling is a vital resource to generate PB, so we choose any pair of degenerate quasi-static normal optical modes ($a_{\mathrm{L},+}$ and $a_{\mathrm{R},+}$, or $a_{\mathrm{L},-}$ and $a_{\mathrm{R},-}$) to generate the strong direction-dependent quadratic optomechanical interaction. In the following, a_{L} and a_{R} are used to denote two optical modes with frequency $\omega_{c_j} = \omega_{j+}$ or ω_{j-}, which describes the case that the driving field propagates from port 1 and port 2, respectively. For instance, when a strong driving field with amplitude ε_{p} and frequency $\omega_{\mathrm{L}} \sim \omega_{c_j} - 2\omega_m$ is input from port 1 to port 2 to excite the optical mode a_{L}, the nonlinear quadratic optomechanical interaction between a_{L} and the mechanical mode is enhanced. The Hamiltonian of the system in a frame rotating at the driving frequency ω_{L} can be expressed as

$$\begin{aligned} H_{s_1} &= (\Delta_{c_0} - |\Delta_{\mathrm{F}}| + gq^2)a^{\dagger}_{\mathrm{L}}a_{\mathrm{L}} \\ &+ (\Delta_{c_0} + |\Delta_{\mathrm{F}}| + gq^2)a^{\dagger}_{\mathrm{R}}a_{\mathrm{R}} \\ &+ \frac{1}{2}\omega_m(q^2+p^2) + \varepsilon_{\mathrm{p}}(a^{\dagger}_{\mathrm{L}} + a_{\mathrm{L}}), \end{aligned} \tag{11}$$

where $\Delta_{c_0} = \omega_0 + J - \omega_{\mathrm{L}}$.

In the strong-driving regime, we perform the standard linearization procedure, and both optical modes and mechanical modes are split into an average coherent amplitude and a fluctuation term: $a_{\mathrm{L}} \to a_{\mathrm{L}} + \alpha_{\mathrm{L}}, a_{\mathrm{R}} \to a_{\mathrm{R}} + \alpha_{\mathrm{R}}, q \to q_s + q, p \to p_s + p$.

The average coherent values α_{L}, α_{R}, q_s, and p_s can be obtained as

$$\begin{aligned} \alpha_{\mathrm{L}} &= \frac{-2\mathrm{i}\varepsilon_{\mathrm{p}}}{\kappa + 2\mathrm{i}(\Delta_{c_0} - |\Delta_{\mathrm{F}}|)}, \\ \alpha_{\mathrm{R}} &= q_s = p_s = 0. \end{aligned} \tag{12}$$

Introducing the creation and annihilation operators for the mechanical mode with $q = (b+b^{\dagger})/\sqrt{2}, p = \mathrm{i}(b^{\dagger}-b)/\sqrt{2}$, the linearized Hamiltonian becomes

$$\begin{aligned} H_{e_1} &= (\Delta_{c_0} - |\Delta_{\mathrm{F}}|)a^{\dagger}_{\mathrm{L}}a_{\mathrm{L}} + (\Delta_{c_0} + |\Delta_{\mathrm{F}}|)a^{\dagger}_{\mathrm{R}}a_{\mathrm{R}} \\ &+ \omega'_m b^{\dagger}b + \frac{g\alpha_{\mathrm{L}}}{2}(a^{\dagger}_{\mathrm{L}} + a_{\mathrm{L}})(b^{\dagger}+b)^2 \\ &+ \frac{g}{2}|\alpha_{\mathrm{L}}|^2(b^2 + b^{\dagger 2}), \end{aligned} \tag{13}$$

where the effective mechanical frequency is $\omega'_m = \omega_m + g|\alpha_{\mathrm{L}}|^2$.

Under the near resonance condition $|\Delta_{c_0} - |\Delta_{\mathrm{F}}|| \ll \omega'_m$, and making the rotating-wave approximation in the case of $G \ll \omega'_m$, the Hamiltonian is described as

$$\begin{aligned} H_{e_2} &= (\Delta_{c_0} - |\Delta_{\mathrm{F}}|)a^{\dagger}_{\mathrm{L}}a_{\mathrm{L}} + (\Delta_{c_0} + |\Delta_{\mathrm{F}}|)a^{\dagger}_{\mathrm{R}}a_{\mathrm{R}} \\ &+ \omega'_m b^{\dagger}b + G(a^{\dagger}_{\mathrm{L}} + a_{\mathrm{L}})(b^{\dagger}b + 1/2), \end{aligned} \tag{14}$$

with the effective optomechanical coupling $G = g\alpha_{\mathrm{L}}$.

Applying the polaron transformation

$$U = \exp[G/(\Delta_{c_0} - |\Delta_{\mathrm{F}}|)(a^{\dagger}_{\mathrm{L}} - a_{\mathrm{L}})(b^{\dagger}b + 1/2)] \tag{15}$$

to the Hamiltonian H_{e_2}, a new Hamiltonian $H_{e_3} = UH_{e_2}U^{\dagger}$ can be calculated as

$$\begin{aligned} H_{e_3} &= (\Delta_{c_0} - |\Delta_{\mathrm{F}}|)a^{\dagger}_{\mathrm{L}}a_{\mathrm{L}} + (\Delta_{c_0} + |\Delta_{\mathrm{F}}|)a^{\dagger}_{\mathrm{R}}a_{\mathrm{R}} \\ &+ (\omega'_m - \Delta_{\mathrm{g}_1})b^{\dagger}b - \Delta_{\mathrm{g}_1}(b^{\dagger}b)^2, \end{aligned} \tag{16}$$

where $\Delta_{\mathrm{g}_1} = \frac{G^2}{\Delta_{c_0} - |\Delta_{\mathrm{F}}|}$. The polaron transformation U is an exact unitary transformation, mathematically valid for any nonzero detuning $\Delta_{c_0} - |\Delta_{\mathrm{F}}| \neq 0$, and it completely eliminates the linear coupling term. The validity of this transformation

CPB Online In-Press

relies on the rotating-wave approximation (requiring $G \ll \omega_m'$) and the linearization procedure made earlier.

Similarly, when the driving field transports in the opposite direction, the linearized Hamiltonian of the system is

$$\begin{aligned} H_{s_2} &= (\Delta_{c_0} - |\Delta_{\rm F}|)a_{\rm L}^\dagger a_{\rm L} + (\Delta_{c_0} + |\Delta_{\rm F}|)a_{\rm R}^\dagger a_{\rm R} \\ &\quad + \omega_m' b^\dagger b + G(a_{\rm R}^\dagger + a_{\rm R})(b^\dagger b + 1/2). \end{aligned} \tag{17}$$

After the polaron transformation, we obtain

$$\begin{aligned} H_{e_4} &= (\Delta_{c_0} - |\Delta_{\rm F}|)a_{\rm L}^\dagger a_{\rm L} + (\Delta_{c_0} + |\Delta_{\rm F}|)a_{\rm R}^\dagger a_{\rm R} \\ &\quad + (\omega_m' - \Delta_{\rm g_2})b^\dagger b - \Delta_{\rm g_2}(b^\dagger b)^2, \end{aligned} \tag{18}$$

where $\Delta_{\rm g_2} = \frac{G^2}{\Delta_{c_0}+|\Delta_{\rm F}|}$.

It is clear that the Hamiltonian H_{e_3} satisfies

$$H_{e_3}|n,m\rangle = E_{n,m}|n,m\rangle, \tag{19}$$

where $|n,m\rangle$ represents the eigenstates of the system with n-photon and m-phonon, and $E_{n,m}$ are the corresponding eigenvalues with

$$E_{n,m} = (\Delta_{c_0} - |\Delta_{\rm F}|)n + (\omega_m' - \Delta_{\rm g_1})m - \Delta_{\rm g_1} m^2. \tag{20}$$

We apply $\tilde{H} = UH_{e_3}U^\dagger$ into Eq. (19), and one can obtain

$$\tilde{H}|\tilde{n},m\rangle = E_{n,m}|\tilde{n},m\rangle, \tag{21}$$

the phonon-dependent displaced number state $|\tilde{n}(m)\rangle$ is given as

$$|\tilde{n},m\rangle = \exp\left[\frac{G}{\Delta_{c_0} - |\Delta_{\rm F}|}(m+1/2)(a - a^\dagger)\right]|n\rangle. \tag{22}$$

To investigate the phonon statistical properties of the mechanical mode, the mechanical mode is driven by a weak pumping field (frequency $\omega_{\rm p}$ and amplitude ε_b). The realization of the pumping for the mechanical mode has been implemented by a dc voltage source,[52] or piezoelectric radio signal,[53] with the corresponding Hamiltonian

$$H_{\rm p} = \varepsilon_b(b\,{\rm e}^{{\rm i}\omega_{\rm p}t} + b^\dagger\,{\rm e}^{-{\rm i}\omega_{\rm p}t}). \tag{23}$$

It can be seen from Eq. (20) that the Kerr-type interaction between phonons with strength $\Delta_{\rm g_1}$ results in the anharmonic energy levels of the system in the few-phonon subspace. When the single-phonon resonant condition $\Delta_{\rm p} = \omega_m' - \omega_{\rm p} = 2\Delta_{\rm g_1}$ is satisfied, the nonresonance results in the suppression of two-phonon transition, that is, the second phonon is blockaded, so the PB is achievable.

Including the decay rate $\kappa_{\rm L}$ ($\kappa_{\rm R}$) of the cavity mode $a_{\rm L}$ ($a_{\rm R}$) and the dissipation γ_m of the mechanical mode, the dynamics of the system can be described by the master equation

$$\begin{aligned} \dot{\rho} &= -{\rm i}[H_t, \rho] + \frac{\kappa_{\rm L}}{2}(2a_{\rm L}\rho a_{\rm L}^\dagger - a_{\rm L}^\dagger a_{\rm L}\rho - \rho a_{\rm L}^\dagger a_{\rm L}) \\ &\quad + \frac{\kappa_{\rm R}}{2}(2a_{\rm R}\rho a_{\rm R}^\dagger - a_{\rm R}^\dagger a_{\rm R}\rho - \rho a_{\rm R}^\dagger a_{\rm R}) \\ &\quad + \frac{\gamma_m}{2}n_m(2b^\dagger\rho b - bb^\dagger\rho - \rho bb^\dagger) \\ &\quad + \frac{\gamma_m}{2}(n_m+1)(2b\rho b^\dagger - b^\dagger b\rho - \rho b^\dagger b), \end{aligned} \tag{24}$$

where the effective Hamiltonian H_t in the rotating frame at $\omega_{\rm p}$ is given by

$$\begin{aligned} H_t &= (\Delta_{c_0} - |\Delta_{\rm F}|)a_{\rm L}^\dagger a_{\rm L} + (\Delta_{c_0} + |\Delta_{\rm F}|)a_{\rm R}^\dagger a_{\rm R} \\ &\quad + \Delta_{\rm p} b^\dagger b + G(a_{\rm L}^\dagger + a_{\rm L})(b^\dagger b + 1/2) \\ &\quad + \varepsilon_b(b + b^\dagger) \end{aligned} \tag{25}$$

for a driving field of the WGM resonator transporting from port 1 to port 2, and

$$\begin{aligned} H_t &= (\Delta_{c_0} - |\Delta_{\rm F}|)a_{\rm L}^\dagger a_{\rm L} + (\Delta_{c_0} + |\Delta_{\rm F}|)a_{\rm R}^\dagger a_{\rm R} \\ &\quad + \Delta_{\rm p} b^\dagger b + G(a_{\rm R}^\dagger + a_{\rm R})(b^\dagger b + 1/2) \\ &\quad + \varepsilon_b(b + b^\dagger) \end{aligned} \tag{26}$$

for a driving field of the WGM resonator transporting from port 2 to port 1, respectively.

The equal-time second-order correlation function $g^{(2)}(0)$ characterizing the phonon statistical properties of the mechanical mode can be calculated as

$$g^{(2)}(0) = \frac{{\rm Tr}(b^{\dagger 2}b^2\rho)}{{\rm Tr}(b^\dagger b\rho)} = \frac{\langle b^{\dagger 2}b^2\rangle}{\langle b^\dagger b\rangle^2}. \tag{27}$$

Here $g^{(2)}(0) < 1$ characterizes PB via sub-Poisson statistics of the phonons, and the limit $g^{(2)}(0) \to 0$ indicates the emergence of strong PB.

3. The realization of the nonreciprocal phonon blockade

Next, we use $\Delta_{\rm F} < 0$ and $\Delta_{\rm F} > 0$ to denote the driving field of the WGM resonator propagating along and against the direction of the spinning optical resonator, respectively, i.e., the driving light travelling from port 1 to port 2 and from port 2 to port 1, respectively. We assume $\kappa_{\rm L} = \kappa_{\rm R}$ and use experimentally feasible parameters,[54–61] that is, $\lambda = 1550$ nm, $Q_{\rm L} = 3\times10^7$, $r = 0.25$ mm, $n_1 = 1.44$, $\kappa_{\rm L} = \omega_0/Q_{\rm L}$, $G = 3\kappa_{\rm L}$, $\gamma_m = 0.1\kappa_{\rm L}$, $\varepsilon_{\rm p} = 0.1\kappa_{\rm L}$, $\Delta_{c_0} = 10\kappa_{\rm L}$, and $\Omega = 70$ kHz.

The optical quality factor $Q_{\rm L} = 3\times10^7$ corresponds to experimentally achieved values for high-quality whispering-gallery microcavities,[54] which determines the optical mode decay rate $\kappa_{\rm L} \approx 2\pi\times6.45$ MHz, providing a low-dissipation environment for quantum optomechanical interactions. The effective optomechanical coupling strength $G = 3\kappa_{\rm L}$ satisfies the strong coupling condition $G > \kappa_{\rm L}$, and can be achieved with moderate pump power in existing experimental systems.[55] The mechanical dissipation rate $\gamma_m = 0.1\kappa_{\rm L}$ satisfies the resolved-sideband condition $\gamma_m < \kappa_{\rm L}$, ensuring that

CPB Online In-Press

the mechanical mode has sufficient coherence time to observe phonon blockade effects.[56,57] The choice of optical pump intensity $\varepsilon_{\rm p}=0.1\kappa_{\rm L}$ and $\Delta_{c_0}=10\kappa_{\rm L}$ aims to achieve stable intracavity field enhancement while maintaining the validity of the linearized treatment of the system. The selection of the rotation angular velocity $\Omega=70$ kHz is based on the following considerations: according to the Sagnac frequency shift in Eq. (1), this angular velocity corresponds to $\Delta_{\rm F}$ on the order of MHz, which is sufficient to introduce a significant nonreciprocal frequency shift in the optical mode, thereby breaking the time-reversal symmetry of the system. This rotation speed falls within the experimentally achievable range of 1 kHz to GHz for microcavity rotation,[45,61] ensuring significant physical effects while maintaining experimental feasibility. Ω modulates the nonlinear strength $\Delta_{\rm g}$ through $\Delta_{\rm F}$, thereby influencing the resonance condition of PB and enabling direction-dependent quantum control.

The second-order correlation function $g^{(2)}(0)$ is shown in Fig. 2 as a function of $\Delta_{\rm p}/\Delta_{\rm g}$ with $\Delta_{\rm g}=G^2/\Delta_{c_0}$. It is clear that the nonreciprocal phonon antibunching and phonon bunching can be achieved when the WGM resonator is spinning. For a stationary WGM resonator, this nonreciprocity vanishes regardless of the direction of the driving light. The physical mechanism for the emergence of several peaks and dips in Fig. 2 can be explained as follows. The dips D_0 and D_1 correspond to the PB in the $n_2(n_2=0,1)$-photon sidebands, which arise from the single-phonon transitions between the vacuum state $|\tilde{0}(0)\rangle|0\rangle$ and the single-phonon state $|\tilde{n_2}(1)\rangle|1\rangle$. Under this condition, the driving condition of the weak mechanical pump field satisfies $\omega_{\rm p}=E_{n_2,1}-E_{0,0}$. For a driving field of the WGM resonator transporting from port 1 to port 2, this driving condition can be written as $\Delta_{\rm p}/\Delta_{\rm g_1}=2-n_2(\frac{\Delta_{c_0}-|\Delta_{\rm F}|}{G})^2$, i.e., $\Delta_{\rm p}/\Delta_{\rm g}=[2-n_2(\frac{\Delta_{c_0}-|\Delta_{\rm F}|}{G})^2]\frac{\Delta_{c_0}}{\Delta_{c_0}-|\Delta_{\rm F}|}$, where $\Delta_{\rm g}=\frac{G^2}{\Delta_{c_0}}$. The peaks P_{n_3} $(n_3=0,1,2)$ correspond to the two-phonon transition between the vacuum state $|\tilde{0}(0)\rangle|0\rangle$ and the two-phonon state $|\tilde{n}_3(2)\rangle|2\rangle$, where the driving condition satisfies $2\omega_{\rm p}=E_{n_3,2}-E_{0,0}$, i.e., $\Delta_{\rm p}/\Delta_{\rm g}=[3-\frac{n_3(\Delta_{c_0}-|\Delta_{\rm F}|)^2}{2G^2}]\frac{\Delta_{c_0}}{\Delta_{c_0}-|\Delta_{\rm F}|}$. In addition, as shown in Fig. 2, selecting $\Omega=70$ kHz yields a clear nonreciprocal peak shift in the $g^{(2)}(0)$ spectrum while remaining within the stable operational range of current experimental techniques. Therefore, we have chosen this value as the primary parameter.

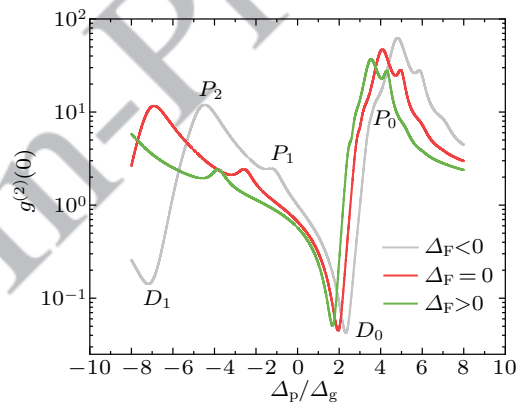


Fig. 2. The second-order correlation function $g^{(2)}(0)$ versus the frequency detuning $\Delta_{\rm p}/\Delta_{\rm g}$ for different driving directions. The other parameters are $\lambda=1550$ nm, $Q_{\rm L}=3\times10^7$, $r=0.25$ mm, $n_1=1.44$, $\kappa_{\rm L}=\omega_c/Q_{\rm L}$, $G=3\kappa_{\rm L}$, $\gamma_m=0.1\kappa_{\rm L}$, $\varepsilon_{\rm p}=0.1\kappa_{\rm L}$, $\Delta_{c_0}=10\kappa_{\rm L}$, $n_m=0$, and $\Omega=70$ kHz. Here we denote $\Delta_{\rm g}=G^2/\Delta_{c_0}$.

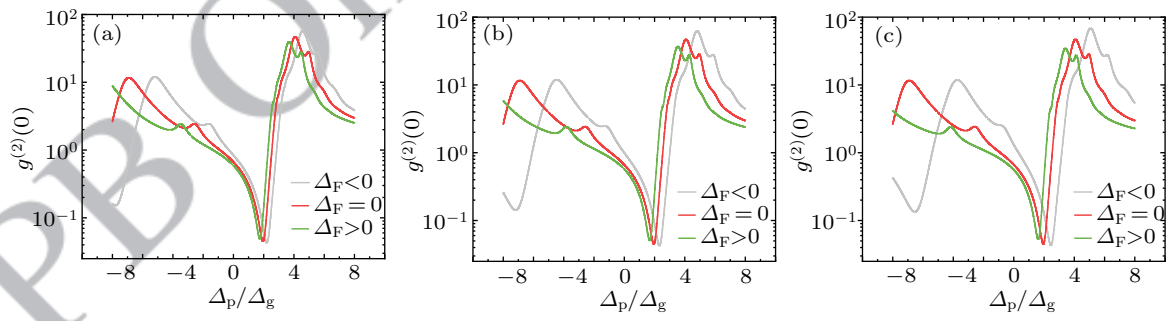


Fig. 3. The second-order correlation function $g^{(2)}(0)$ versus the frequency detuning $\Delta_{\rm p}/\Delta_{\rm g}$ for different driving directions at various angular velocities Ω: (a) $\Omega=50$ kHz, (b) $\Omega=70$ kHz and (c) $\Omega=90$ kHz. All other parameters are the same as those in Fig. 2.

Similarly, when the driving field of the WGM resonator transports from port 2 to port 1, the driving conditions for single-phonon and two-phonon transitions are

$$\Delta_{\rm p}/\Delta_{\rm g}=\left[2-n_2\left(\frac{\Delta_{c_0}+|\Delta_{\rm F}|}{G}\right)^2\right]\frac{\Delta_{c_0}}{\Delta_{c_0}+|\Delta_{\rm F}|},$$
$$\Delta_{\rm p}/\Delta_{\rm g}=\left[3-\frac{n_3(\Delta_{c_0}+|\Delta_{\rm F}|)^2}{2G^2}\right]\frac{\Delta_{c_0}}{\Delta_{c_0}+|\Delta_{\rm F}|}.$$

The reason for the generation of nonreciprocal PB is that the Sagnac effect induced by the rotation of WGM resonator breaks the time-reversal symmetry of the optomechanical system. The irreversible resonance wavelength subsequently affects the resonance conditions under which PB occurs. The differences in values of the peaks and dips in the curves of $g^{(2)}(0)$ for different driving directions primarily originate from the other photon-assisted phonon transitions which can also happen at the same detuning $\Delta_{\rm p}/\Delta_{\rm g}$ and ratio Δ_{c_0}/G.

It can be seen from Fig. 2 that the rotation of the WGM resonator is necessary for the generation of the nonreciprocal PB. Next we further investigate the dependence of the second-

CPB Online In-Press

order correlation function $g^{(2)}(0)$ on the angular velocity Ω of the rotation of the WGM resonator. As shown in Fig. 3, we plot the second-order correlation function $g^{(2)}(0)$ versus the frequency detuning Δ_p/Δ_g for different driving directions at various angular velocities Ω. It is found that the frequency detuning region of the mechanical pump field where the nonreciprocal PB emerges can be broadened effectively with the increase of Ω. $g^{(2)}(0)$ shifts linearly with Ω; an obvious blue shift and red shift exist for $\Delta_F < 0$ and $\Delta_F > 0$, respectively. The result shows that the nonreciprocal PB can be effectively modulated by Ω.

Environmental temperature is a crucial physical quantity in the investigation of quantum effects. We now plot $g^{(2)}(0)$ versus the frequency detuning Δ_p/Δ_g with different thermal phonon numbers n_m for different driving directions in Fig. 4. Obviously, the nonreciprocal PB can still exist when the thermal phonon noises are considered. The thermal phonon numbers have a negative impact on $g^{(2)}(0)$, and the nonreciprocal PB will be destroyed with the increasing n_m. A low temperature environment is beneficial for the preparation of nonreciprocal PB.

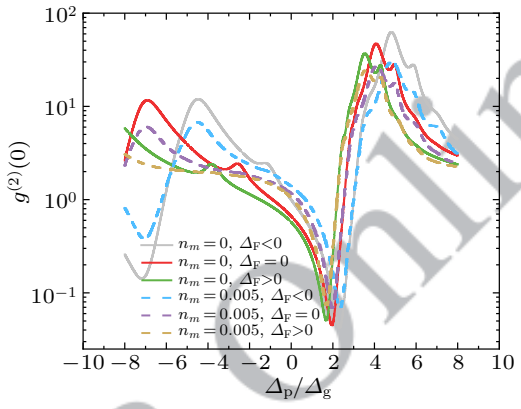


Fig. 4. The second-order correlation function $g^{(2)}(0)$ versus the frequency detuning Δ_p/Δ_g with different thermal phonon numbers n_m for different driving directions. All other parameters are the same as those in Fig. 2.

In this scheme, the anharmonic energy level of the system is the physical origin of the generation of the PB, and the effective optomechanical coupling G is a key factor used to generate the nonlinear interaction between phonons which leads to the emergence of the anharmonic energy level. Therefore, we show the contour plots of $g^{(2)}(0)$ in logarithmic scale [i.e., $\log_{10} g^{(2)}(0)$] as a function of G/κ_L and Δ_p/Δ_g when the WGM resonator is stationary. From Fig. 5, it can be found that the optimal PB occurs exactly at the point $\Delta_p = 4.02\kappa_L$, $G = 4.48\kappa_L$, which corresponds to the dip D_0 where the driving condition $\Delta_p = 2\Delta_g$ of 0-photon-assisted single-phonon transition is satisfied. G can be altered by the driving field of the optical mode a_L (a_R) and the tunneling coupling J when $\Delta_F < 0$ ($\Delta_F > 0$) according to Eqs. (8) and (12) when the WGM resonators are spinning. Our result also shows that the driving on cavity mode and the tunneling coupling between cavity modes are useful tools to control the nonreciprocal PB.

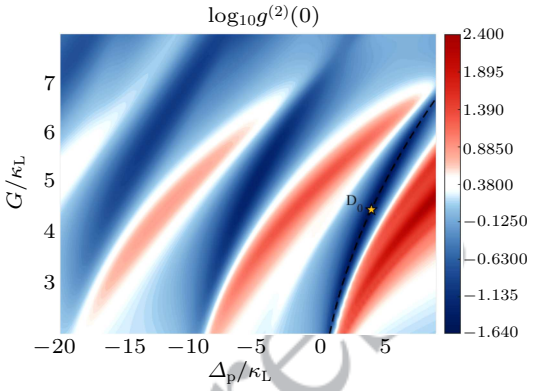


Fig. 5. The second-order correlation function $\log_{10} g^{(2)}(0)$ versus the frequency detuning Δ_p/κ_L and the effective optomechanical coupling strength G/κ_L. Here we set $\Delta_F = 0$, all other parameters are the same as those in Fig. 2.

Next, we will demonstrate the experimental feasibility of this scheme. The nonreciprocal PB mechanism proposed in this study possesses a solid foundation for future experimental validation. The core platform of rotating optical microcavities has already been experimentally demonstrated. For example, an air-bearing technique was utilized to realize stable kHz-range rotation of a millimeter-scale silica sphere, with an optical nonreciprocal effect successfully observed in the process.[46] The underlying Sagnac effect and integrated whispering-gallery microcavity platform relied upon by this technical scheme have been conceptually extended and validated in other nonreciprocal devices, such as optical circulators.[62] Concurrently, our proposal is grounded in feasibility at the more complex level of hybrid optomechanical systems. On one hand, the high-quality-factor ($Q > 10^8$) silica whispering-gallery microcavities required to construct the system represent a mature experimental platform.[63] More importantly, the central concept of applying nonreciprocal effects to a tri-mode hybrid system that couples two optical modes with one mechanical mode has received clear support in relevant theoretical research. For instance, within the framework of rotating microcavities, nonreciprocity has been successfully theoretically extended to phononic quantum devices like phonon lasers.[35–39]

Furthermore, in static on-chip optomechanical systems, the core configuration, where two optical cavities are coupled via a shared nanomechanical oscillator, has been detailed in terms of numerical verification and principle design. It serves as a fundamental building block for scalable optomechanical arrays on platforms such as photonic crystals.[64] This directly supports the theoretical extension in this work combining rotation-induced nonreciprocity with complex coupled optomechanical models. Regarding measurement and characterization, the key signature of PB, which is strong sub-

CPB Online In-Press

Poissonian phonon statistics, can be detected via measurements of the second-order correlation function of mechanical motion. Therefore, despite challenges in system integration and precise control, the physical mechanisms, critical components, and technical pathways involved in this scheme have all received principle-level validation in related experiments or theories, laying a solid groundwork for future experimental realization.

4. Conclusion

In summary, we propose a scheme for realizing the nonreciprocal PB in a spinning optomechanical system composed of one mechanical resonator optomechanically coupled to two optical resonators, i.e., PB can be generated when the system is driven from one direction but not from the other. The nonreciprocal PB originates from the anharmonic energy level of the system and the Sagnac effect induced by the rotation of two optical resonators. The direction-dependent mechanical frequency detuning region where the nonreciprocal PB occurs can be broadened with the increase of the angular velocities of two optical resonators. The strong PB can be obtained when a proper optomechanical coupling strength and frequency detuning between the mechanical mode and the pump field are adjusted. Moreover, the nonreciprocal PB can still exist when the mechanical thermal phonon numbers are considered. Our proposal provides a feasible method to control the quantum properties of the mechanical oscillators. The realization of the nonreciprocal PB device presented in our scheme opens new possibilities for quantum information processing based on phonons and sensitive measurements.

Acknowledgements

This work is supported by the Scientific and Technological Research Program of Chongqing Municipal Education Commission (Grant No. KJQN202400624), the Natural Science Foundation of Chongqing, China (Grant Nos. CSTB2024NSCQ-MSX0880 and CSTB2024NSCQ-MSX1187), and the Research Institute of Intelligent Manufacturing Industry Technology of SiChuan Arts and Science university (Grant No. ZNZZ2501).

References

[1] O'Connell A D, Hofheinz M, Ansmann M, Bialczak R C, Lenander M, Lucero E, Neeley M, Sank D, Wang H, Weides M, *et al.* 2010 *Nature* **464** 697
[2] Reed A, Mayer K, Teufel J, Burkhart L, Pfaff W, Reagor M, Sletten L, Ma X, Schoelkopf R, Knill E, *et al.* 2017 *Nat. Phys.* **13** 1163
[3] Chu Y, Kharel P, Renninger W H, Burkhart L D, Frunzio L, Rakich P T and Schoelkopf R J 2017 *Science* **358** 199
[4] Tomes M and Carmon T 2009 *Phys. Rev. Lett.* **102** 113601
[5] Kippenberg T J and Vahala K J 2008 *Science* **321** 1172
[6] Zwickl B, Shanks W, Jayich A, Yang C, Bleszynski Jayich A, Thompson J and Harris J 2008 *Appl. Phys. Lett.* **92** 103125
[7] Marquardt F and Girvin S M 2009 *Physics* **2** 40
[8] Aspelmeyer M, Meystre P and Schwab K 2012 *Phys. Today* **65** 29
[9] Chen S S, Zhang J J, Li J N, Zhang N N, Guo Y R and Yang H 2024 *Chin. Phys. B* **33** 110305
[10] Chen L T, Qin L G, Tian L J, Huang J H, Zhou N R and Gong S Q 2024 *Chin. Phys. B* **33** 064204
[11] Imamoğlu A, Schmidt H, Woods G and Deutsch M 1997 *Phys. Rev. Lett.* **79** 1467
[12] Miranowicz A, Bajer J, Lambert N, Liu Y X and Nori F 2016 *Phys. Rev. A* **93** 013808
[13] Wang X, Miranowicz A, Li H R and Nori F 2016 *Phys. Rev. A* **93** 063861
[14] Ramos T, Sudhir V, Stannigel K, Zoller P and Kippenberg T J 2013 *Phys. Rev. Lett.* **110** 193602
[15] Xie H, Liao C G, Shang X, Ye M Y and Lin X M 2017 *Phys. Rev. A* **96** 013861
[16] Wang Y, Wu J L, Han J X, Xia Y, Jiang Y Y and Song J 2022 *Phys. Rev. Appl.* **17** 024009
[17] Aspelmeyer M, Kippenberg T J and Marquardt F 2014 *Rev. Mod. Phys.* **86** 1391
[18] Chen S S, Zhang H, Ai Q and Yang G J 2019 *Phys. Rev. A* **100** 052306
[19] Seok H and Wright E 2017 *Phys. Rev. A* **95** 053844
[20] Zhu G L, Lü X Y, Wan L L, Yin T S, Bin Q and Wu Y 2018 *Phys. Rev. A* **97** 033830
[21] Zheng L L, Yin T S, Bin Q, Lü X Y and Wu Y 2019 *Phys. Rev. A* **99** 013804
[22] Yuan N, He S, Li S Y, Wang N and Zhu A D 2023 *Opt. Express* **31** 20160
[23] Xu Y J and Xie H 2024 *Front. Phys.* **19** 32202
[24] Auld B A 1959 *IEEE Trans. Microw. Theory Tech.* **7** 238
[25] Milano U, Saunders J H and Davis L 1960 *IRE Trans. Microw. Theory Tech.* **8** 346
[26] Hadad Y and Steinberg B Z 2010 *Phys. Rev. Lett.* **105** 233904
[27] Bi L, Hu J, Jiang P, Kim D H, Dionne G F, Kimerling L C and Ross C 2011 *Nat. Photon.* **5** 758
[28] Sounas D L, Caloz C and Alu A 2013 *Nat. Commun.* **4** 2407
[29] Estep N A, Sounas D L, Soric J and Alu A 2014 *Nat. Phys.* **10** 923
[30] Sounas D and Alù A 2014 *8th International Congress METAMATERIALS* 415
[31] Viola G and DiVincenzo D P 2014 *Phys. Rev. X* **4** 021019
[32] Chen S S, Meng S S, Deng H and Yang G J 2021 *Ann. Phys. (Berl.)* **533** 2000343
[33] Guo Q, Zhou K X, Bai C H, Zhang Y, Li G and Zhang T 2023 *Phys. Rev. A* **108** 033515
[34] Zhao B, Zhou K X, Wei M R, Cao J and Guo Q 2024 *Opt. Lett.* **49** 486
[35] Jiang Y, Maayani S, Carmon T, Nori F and Jing H 2018 *Phys. Rev. Appl.* **10** 064037
[36] Lu T X, Wang Y, Xia K, Xiao X, Kuang L M and Jing H 2024 *Sci. China Phys. Mech. Astron.* **67** 260312
[37] Xu H, Jiang L, Clerk A and Harris J 2019 *Nature* **568** 65
[38] Lai D G, Huang J F, Yin X L, Hou B P, Li W, Vitali D, Nori F and Liao J Q 2020 *Phys. Rev. A* **102** 011502
[39] Lai D G, Miranowicz A and Nori F 2024 *Phys. Rev. Lett.* **132** 243602
[40] Huang R, Miranowicz A, Liao J Q, Nori F and Jing H 2018 *Phys. Rev. Lett.* **121** 153601
[41] Xie H, He L W, Shang X, Lin G W and Lin X M 2022 *Phys. Rev. A* **106** 053707
[42] Liu Y M, Cheng J, Wang H F and Yi X 2023 *Opt. Express* **31** 12847
[43] Yao X Y, Ali H, Li F L and Li P B 2022 *Phys. Rev. Appl.* **17** 054004
[44] Xu X, Zhao Y, Wang H, Jing H and Chen A 2020 *Photon. Res.* **8** 143
[45] Malykin G B 2000 *Phys. Usp.* **43** 1229
[46] Maayani S, Dahan R, Kligerman Y, Moses E, Hassan A U, Jing H, Nori F, Christodoulides D N and Carmon T 2018 *Nature* **558** 569
[47] Heinrich G, Harris J and Marquardt F 2010 *Phys. Rev. A* **81** 011801
[48] Wu H, Heinrich G and Marquardt F 2013 *New J. Phys.* **15** 123022
[49] Paraïso T K, Kalaee M, Zang L, Pfeifer H, Marquardt F and Painter O 2015 *Phys. Rev. X* **5** 041024
[50] Xie H, Liao C G, Shang X, Chen Z H and Lin X M 2018 *Phys. Rev. A* **98** 023819
[51] Zhang J S, Li M C and Chen A X 2019 *Phys. Rev. A* **99** 013843
[52] Szorkovszky A, Brawley G A, Doherty A C and Bowen W P 2013 *Phys. Rev. Lett.* **110** 184301
[53] Fan L, Fong K Y, Poot M and Tang H X 2015 *Nat. Commun.* **6** 5850

CPB Online-First

[54] Peng B, Özdemir Ş K, Lei F, Monifi F, Gianfreda M, Long G L, Fan S, Nori F, Bender C M and Yang L 2014 *Nat. Phys.* **10** 394

[55] Ding L, Baker C, Senellart P, Lemaitre A, Ducci S, Leo G and Favero I 2011 *Appl. Phys. Lett.* **98** 113108

[56] Verhagen E, Deléglise S, Weis S, Schliesser A and Kippenberg T J 2012 *Nature* **482** 63

[57] Teufel J D, Donner T, Li D, Harlow J W, Allman M, Cicak K, Sirois A J, Whittaker J D, Lehnert K W and Simmonds R W 2011 *Nature* **475** 359

[58] Vahala K J 2003 *Nature* **424** 839

[59] Huet V, Rasoloniaina A, Guillemé P, Rochard P, Féron P, Mortier M, Levenson A, Bencheikh K, Yacomotti A and Dumeige Y 2016 *Phys. Rev. Lett.* **116** 133902

[60] Reimann R, Doderer M, Hebestreit E, Diehl R, Frimmer M, Windey D, Tebbenjohanns F and Novotny L 2018 *Phys. Rev. Lett.* **121** 033602

[61] Ahn J, Xu Z, Bang J, Deng Y H, Hoang T M, Han Q, Ma R M and Li T 2018 *Phys. Rev. Lett.* **121** 033603

[62] Shen Z, Zhang Y L, Chen Y, Sun F W, Zou X B, Guo G C, Zou C L and Dong C H 2018 *Nat. Commun.* **9** 1797

[63] Zhou X, Li J, Wang M, Lei Y, Cheng Y, Wang Z, Zhang Z, Li Z, Zhang H, Xiao Z et al. 2025 *Photonics Res.* **13** 3172

[64] Tian F and Notomi M 2024 *Opt. Mater. Express* **14** 2239

CPB Online In-Press